Advanced Solid State NMR Techniques for the Characterization of Sol–Gel-Derived Materials

CHRISTIAN BONHOMME,* CRISTINA COELHO, NIKI BACCILE, CHRISTEL GERVAIS, THIERRY AZAÏS, AND FLORENCE BABONNEAU
Université Pierre et Marie Curie-Paris 6, CNRS UMR 7574, Laboratoire Chimie de la Matière Condensée de Paris, Paris, F-75005 France

ABSTRACT

A large array of advanced solid state NMR (nuclear magnetic resonance) techniques is presented in the frame of the structural characterization of sol–gel-derived materials. These techniques include the pertinent detection of ^{17}O chemical shifts, MAS (magic angle spinning) J spectroscopy in the solid state, high-resolution ^{1}H spectroscopy, heteronuclear and homonuclear D (dipolar)-derived multidimensional correlation experiments, and first-principles calculations of NMR parameters. This spectroscopic approach is suitable for the in-depth description of multicomponent sol–gel derivatives, crystalline and amorphous biocompatible silicophosphates, Al–O–P clusters, and templated porous materials. It offers unique perspectives for the description of the hybrid interfaces in terms of chemical and spatial connectivities.

Introduction

The tailoring of materials obtained by sol–gel methods is now well-established and widely used for a large variety of chemical, physical, and mechanical applications.[1] These materials include (i) numerous silica- and/or siloxane-based hybrid derivatives, (ii) functional organic and inorganic materials involving even biological components, (iii) mesoporous materials synthesized in the presence of surfactants or block copolymers, and (iv) host–guest systems involving immobilized molecules in porous structures. All these systems can be considered as nanocomposites whose physical and chemical properties are related to the homogeneity of the complex oxide network and to the chemical nature of the interfaces between the involved nanocomponents. The characterization of these materials relies on the crucial notion of connectivity, which can be further defined in terms of chemical connectivity and spatial connectivity.

Recent developments in solid state NMR offer appealing perspectives for the detailed characterization of sol–gel materials. This spectroscopic technique, which is a local probe in nature, can establish "dialogs" between nuclear spins for typical lengths ranging from several angstroms to ~100 nm.[2,3] In that sense, solid state NMR is a perfect tool for investigation of the interfaces in nanomaterials. The versatility of the NMR approach relies on the fact that it is possible to "play" with all NMR interactions, namely, the chemical shift (δ), the scalar coupling (J), and the dipolar (D) and quadrupolar (Q; $I > ^1/_2$) interactions, and to predict the NMR parameters by first-principles calculations.

Recently, spectacular improvements in resolution have been achieved for the quadrupolar nuclei and for ^{1}H by using sophisticated methods such as the MQ MAS (multiple-quantum magic angle spinning) experiment[4] and ultrafast MAS,[5] respectively. Quadrupolar nuclei such as ^{27}Al, ^{11}B, and ^{51}V are often present in sol–gel materials and can be considered as spectroscopic spies. ^{17}O ($I = ^5/_2$) is obviously a key nucleus for the description of complex oxide networks, as well as ^{1}H, which is present in all components of the nanocomposite materials. Solid state J spectroscopy offers new opportunities for the description of chemical bonding in solids.[6,7] This approach should be of paramount importance for the description of the covalent nature of grafting on oxide nanoparticles. As we will show below, the δ and J interactions are able to characterize the chemical connectivities between species.

The spatial connectivities can be established by using the dipolar interaction and the spin diffusion process. The CP (cross-polarization) experiment[8] establishes contacts between dipolarly coupled spins. This interaction is proportional to $1/r^3$, where r stands for the internuclear distance. The CP approach is therefore a method of choice for distance measurements and for the characterization of hybrid interfaces through two-dimensional (2D) HETCOR experiments (heteronuclear correlation).[3] The dipolar interaction can be strongly modulated by the mobility of the involved species, leading to crucial dynamical data.

In the case of quadrupolar nuclei, alternative techniques such as TRAPDOR (transfer of population in double resonance)[9] can be implemented, leading also to the estimation of internuclear distances.

The strong $^{1}H–^{1}H$ dipolar interaction is of prime importance for the description of interfaces and can be used for the description of proton spatial connectivities and H-bonded networks. 2D double-quantum (DQ) experiments (BABA or BAck to BAck)[10] allow the selection of $^{1}H–^{1}H$ spin pairs, thereby disentangling complex ^{1}H spectra. The BABA acronym comes from the presence of very closely spaced pulses in the time domain (see Figure 8, bottom).

Christian Bonhomme was born in 1967 and earned his Ph.D. at the Université P. et M. Curie (Paris, France) in 1994, where he is presently Professor.

Cristina Coelho was born in 1981 and is currently preparing her Ph.D. at the Université P. et M. Curie.

Niki Baccile was born in 1978 and earned his Ph.D. at the Université P. et M. Curie in 2006. He at present has a postdoctoral position in Montpellier, France.

Christel Gervais was born in 1973 and earned her Ph.D. at the Université P. et M. Curie in 1999, where she is at present an Assistant Professor.

Thierry Azaïs was born in 1974 and earned his Ph.D. at the Université P. et M. Curie in 2001, where he is at present an Assistant Professor.

Florence Babonneau was born in 1957 and earned her Ph.D. at the Université P. et M. Curie in 1984, where she is at present Directrice de Recherches at the CNRS.
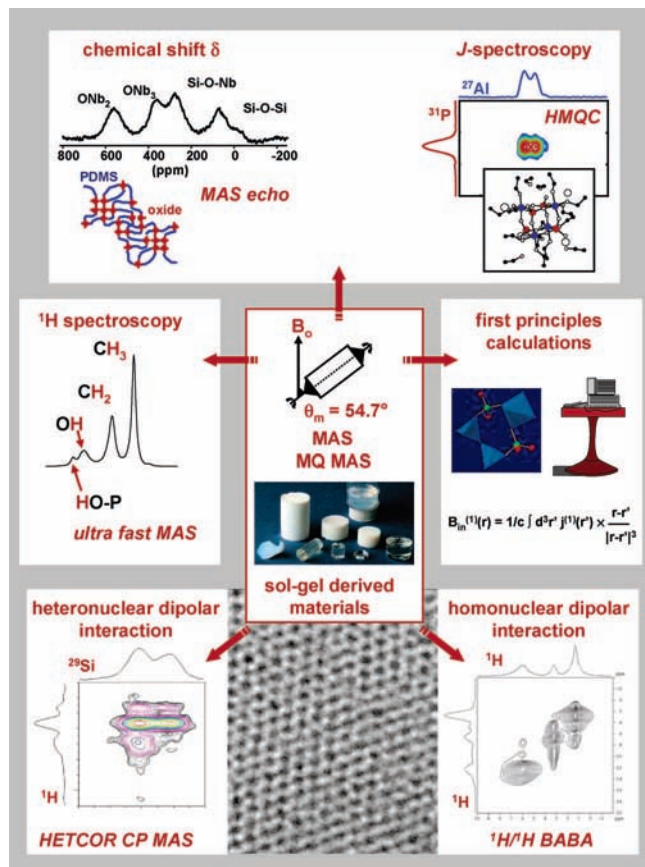
* To whom correspondence should be addressed.

FIGURE 1. Solid state NMR approach presented in this work.

In parallel to this experimental NMR approach, powerful first-principles calculations of NMR parameters[11] can act as an original way of improving the understanding of the spectral data and can be safely transposed to the study of ill-defined interfaces.[12] The various aspects of the solid state NMR approach are summarized in Figure 1. The core of this approach corresponds to high-resolution experiments, namely, MAS and MQ MAS. Starting from these fundamental experiments, we are then able to focus on each NMR interaction with a precise spectroscopic goal in mind, as well as on the computer-assisted calculations of NMR data.

During the past few years, several groups have combined high-resolution ^{1}H NMR spectroscopy [single-quantum (SQ) and DQ], HETCOR experiments (^{1}H–^{29}Si and ^{1}H–^{27}Al), spin diffusion, exchange spectroscopy, and J spectroscopy for the characterization of hybrid materials,[13–16] functionalized nanoparticles,[17,18] and templated porous materials in powder as well as in thin film forms.[19–26]

The aim of this Account is to illustrate the solid state NMR approach applied to the characterization of chemical and spatial connectivities in sol–gel materials. The chemical connectivities will be demonstrated by using the ^{17}O chemical shift as a probe for the study of multicomponent sol–gel materials and by using the MAS J spectroscopy in the case of silicophosphates and aluminophosphate clusters. The silicophosphate gels are potential candidates for biocompatible materials, whereas the Al–O–P clusters can

act as starting materials for aluminophosphate mesoporous materials.[27] The next section deals with ^{1}H high-resolution solid state NMR and CP experiments. Distance measurement is demonstrated in the case of silsesquioxanes, which are precursors for materials with controlled porosity.[28,29] HETCOR and ^{1}H DQ experiments will be presented in the frame of the silica–surfactant interactions in mesophases, whereas TRAPDOR experiments will illustrate the study of silica–hydroxyapatite composites. Finally, first-principles calculations will be applied to the structural characterization of a surfactant-templated silica framework in the absence of three-dimensional (3D) crystallinity.

Chemical Connectivities

Two interactions are considered in this section: the chemical shift (δ) and the scalar coupling J. We will focus on the $\delta(^{17}$O) of oxo bridges in sol–gel derivatives and MAS-J-INADEQUATE (incredible natural abundance double quantum transfer experiment) and MAS-J-HMQC (heteronuclear multiple-quantum correlation) experiments in the frame of silicophosphates and aluminophosphates.

^{17}O MAS NMR Experiments. The degree of homogeneity of the multicomponent sol–gel materials depends on the ability to favor co-condensation reactions between the precursors, despite their intrinsically different reactivities with respect to hydrolysis. Oxygen is a key chemical element in sol–gel chemistry,[30] and ^{17}O solid state NMR experiments appear to be a straightforward characterization tool for probing the different oxo bridges. However, one difficulty with this technique is its poor sensitivity due to the low natural abundance of the ^{17}O isotope (0.037%). This problem can be overcome by using ^{17}O-enriched water for the hydrolysis step that ensures efficient incorporation of ^{17}O into the growing oxide network. Another difficulty results from second-order quadrupolar effects ($I = {}^5/_2$), leading to broadened lines under MAS. Interestingly, ^{17}O NMR chemical shifts are very sensitive to molecular structure and chemical environment. Coordination and bonding of oxygen atoms may be distinguished due to a large chemical shift range ($\approx$1500 ppm), as illustrated in Figure 2a for Si–O–Si,[31] Ti–O–Ti,[32] Zr–O–Zr,[33] Ta–O–Ta,[34] Nb–O–Nb,[35] Ge–O–Ge,[36] V–O–V,[37] Al–O–Al,[38] and B–O–B[39] bonds. Signals from co-condensed Si–O–M species are expected at intermediate chemical shift values between Si–O–Si and M–O–M shifts, as already reported for M = Ti,[40,41] Ta,[34] V,[42] B,[43] Al,[38] Zr, Nb, or Ge.[44]

The ^{17}O MAS NMR spectra of several polydimethylsiloxane (PDMS)–oxide nanocomposites[44] prepared from Me$_2$Si(OEt)$_2$ (dimethyldiethoxysilane) and metal alkoxides M(OR)$_n$, where M = Ti, Zr, Nb, and Ta are presented in Figure 2b. From Figure 2a, self-condensed Si–O–Si ($\sim$0–100 ppm) and M–O–M ($>$250 ppm) bonds are evidenced. Interestingly, several signals are observed for these latter species, corresponding to the multiple coordination modes of O atoms (with transition metal elements). In the intermediate chemical shift range, co-condensed Si–O–M
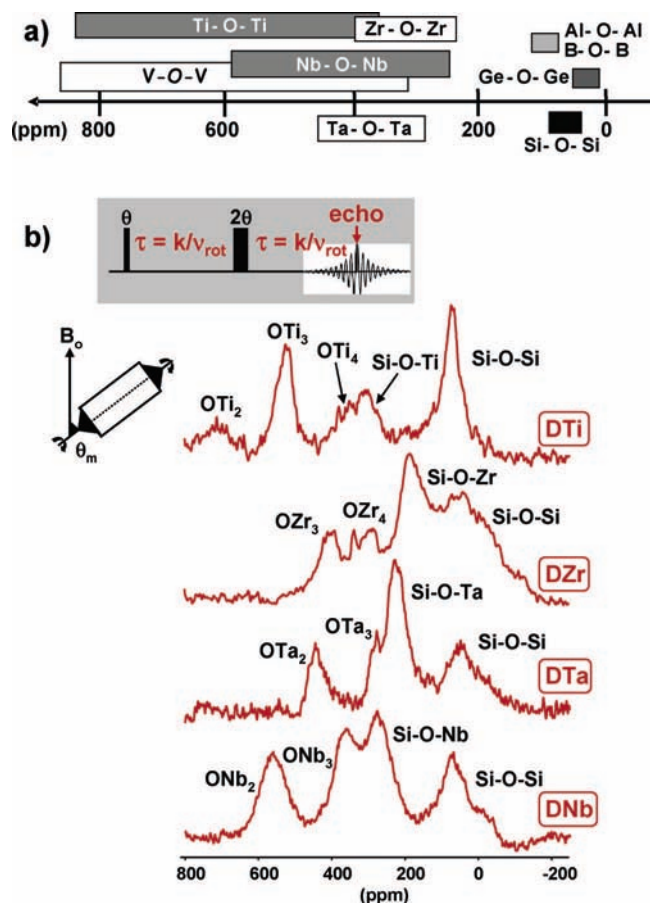
FIGURE 2. (a) ^{17}O isotropic chemical shifts for M–^{17}O–M oxo bridges. (b) ^{17}O MAS echo experiments for several PDMS–metal–oxo nanocomposites.[44]

resonances were observed with large intensities. This proves that good interconnection within the oxide network is attained.

The identification of mixed Si–O–M oxo bridges where M = Al, Ge, or B is more difficult because of overlapping signals (Figure 2a). In this case, the MQ MAS sequence[4] has been succesfully applied to distinguish Si–O–Si from Si–O–B bonds in a polyborosiloxane gel[43] as well as Si–O–Si from Si–O–Al bonds in an aluminosilicate.[38] More difficult is the identification of the various Si–O–Si oxo bridges in siloxane–silica systems because of similar ^{17}O chemical shifts. Nonetheless, using ^{17}O MQ MAS NMR experiments, (T)–O–(T), (T)–O–(Q), and (Q)–O–(Q) units could be distinguished in gels from mixtures of MeSi(OEt)$_3$ and Si(OEt)$_4$[16] (T and Q stand for C-SiO$_3$ and SiO$_4$ units, respectively).

Such ^{17}O studies can be extended to phosphonate materials. Phenylphosphonate-functionalized titania have been studied by ^{17}O MAS NMR,[45] showing the presence of extensive Ti–O–P bonding in the materials.

***J* Spectroscopy in Solid State NMR.** *J*-derived sequences have been extended to the study of crystalline and amorphous derivatives (homonuclear INADEQUATE and heteronuclear HMQC). The facile use of the *J*-derived MAS experiments relies on the fact that the characteristic lifetimes of the involved coherences are long enough for efficient transfer of coherence or polarization.[7,46] Crystal-
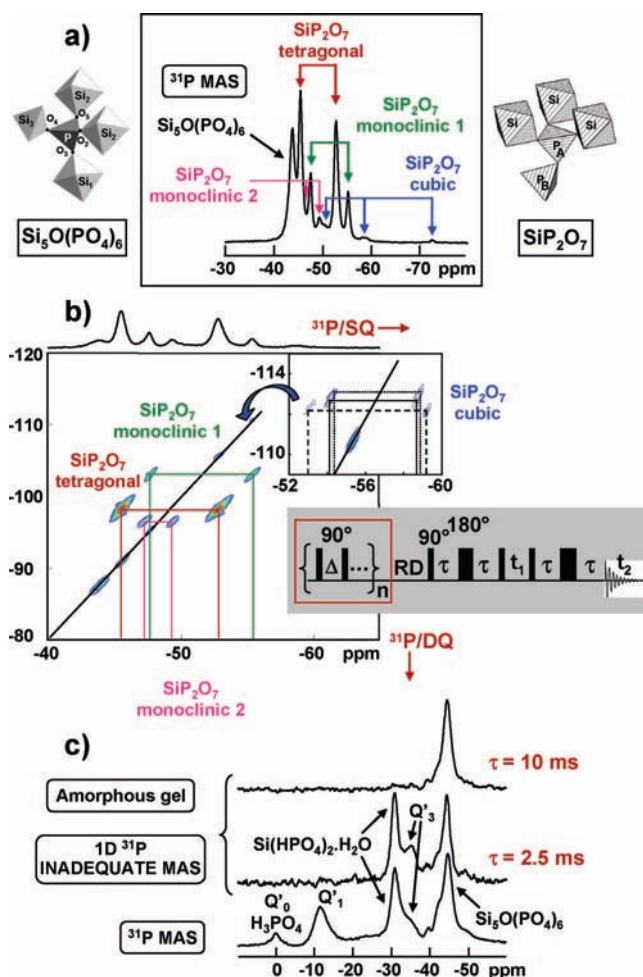
FIGURE 3. (a) ^{31}P MAS spectrum of SiP$_2$O$_7$ polymorphs and Si$_5$O(PO$_4$)$_6$. (b) ^{31}P–^{31}P INADEQUATE. (c) INADEQUATE experiment applied to a silicophosphate gel.[48]

line phosphate phases and amorphous glasses have been characterized by ^{31}P–^{31}P INADEQUATE, ^{31}P *J*-resolved experiments, and HMQC experiments.[7,47] *J* spectroscopy is obviously suitable for the structural characterization of silicophosphates and aluminophosphates, in both the crystalline and amorphous states.[48] Figure 3a shows the ^{31}P MAS spectrum of a complex mixture of SiP$_2$O$_7$ polymorphs and the Si$_5$O(PO$_4$)$_6$ phase[49] (atomic environments are also presented). The ^{31}P–^{31}P homonuclear INADEQUATE spectrum (Figure 3b), based on $^2J_{P-O-P}$ constants (~20 Hz), allows unambiguous assignment of the pairs of atoms (P$_A$ and P$_B$) corresponding to the various phases. Such an experiment correlates a SQ MAS spectrum and a DQ spectrum corresponding to the sum of the individual chemical shifts. The INADEQUATE approach can be extended to amorphous silicophosphate gels. In Figure 3c, the one-dimensional (1D) INADEQUATE spectrum of a gel [1:4:3 Si(OEt)$_4$:EtOH:H$_2$O, H$_4$P$_2$O$_7$, 1:1 Si:P, T = 136 °C] is presented, showing the editing role of the sequence in terms of P–O–P bonds versus τ.[48] Here, the notation Q$'_N$ stands for OP(OP)$_N$(OX)$_{3-N}$ species where $0 \leq N \leq 3$.

Figure 4 illustrates the heteronuclear MAS-*J*-HMQC experiment, characterizing P–O–Si bonds in the complex crystalline and amorphous silicophosphate mixtures.[48,49]
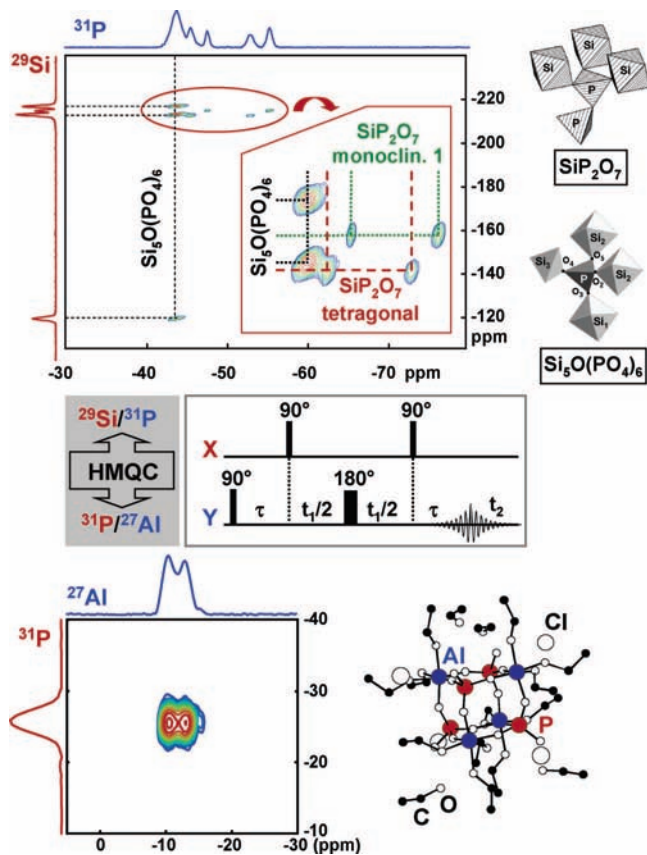
FIGURE 4. (Top) 2D ^{29}Si–^{31}P MAS-*J*-HMQC experiment applied to SiP$_2$O$_7$ polymorphs and Si$_5$O(PO$_4$)$_6$.[49] (Bottom) 2D ^{31}P–^{27}Al MAS-*J*-HMQC experiment applied to [Al$_4$(HPO$_4$)$_4$(C$_2$H$_5$OH)$_{12}$]Cl$_4$·4C$_2$H$_5$OH.[50]

Cross-peaks indicate the chemical connections between the ^{29}Si nuclei and the corresponding pyrophosphate groups or the unique P site in the case of Si$_5$O(PO$_4$)$_6$ ($^2J_{P–O–Si} \sim 15$ Hz).

Various Al–O–P secondary building units (SBU) of zeolites have been described in the literature. [Al$_4$(HPO$_4$)$_4$(C$_2$H$_5$OH)$_{12}$]Cl$_4$·4C$_2$H$_5$OH[50] (shown in Figure 4) can be described as a cubane-shaped cluster, involving Al–O–P and P–OH bonds. The ^{27}Al–^{31}P MAS-*J*-HMQC spectrum shows the correlation between the unique ^{27}Al site (broadened by second-order quadrupolar effects) and the unique ^{31}P site ($^2J_{Al–O–P} \sim 25$ Hz).

Spatial Connectivities

In this section, the homonuclear and heteronuclear dipolar interactions are used for spectroscopic purposes. Such interactions involve mainly ^{1}H, for which adequate high-resolution techniques are required.

^{1}H High-Resolution Solid State NMR. ^{1}H nuclei are mainly subjected to the homogeneous homonuclar dipolar interaction. It follows that standard MAS experiments ($\nu_{rot} \leq 15$ kHz) are generally unable to achieve reasonable resolution. Resolution has been greatly improved over the past few years by a combination of fast MAS,[5] Lee–Goldburg (LG) off-resonance decoupling,[51] multiple-pulse experiments,[52] and tailored pulse schemes.[53] Figure 5a shows the dramatic increase in resolution for [Al$_4$(HPO$_4$)$_4$(C$_2$H$_5$OH)$_{12}$]Cl$_4$·4C$_2$H$_5$OH[50] by using fast MAS ($B_0 = 14$ T).
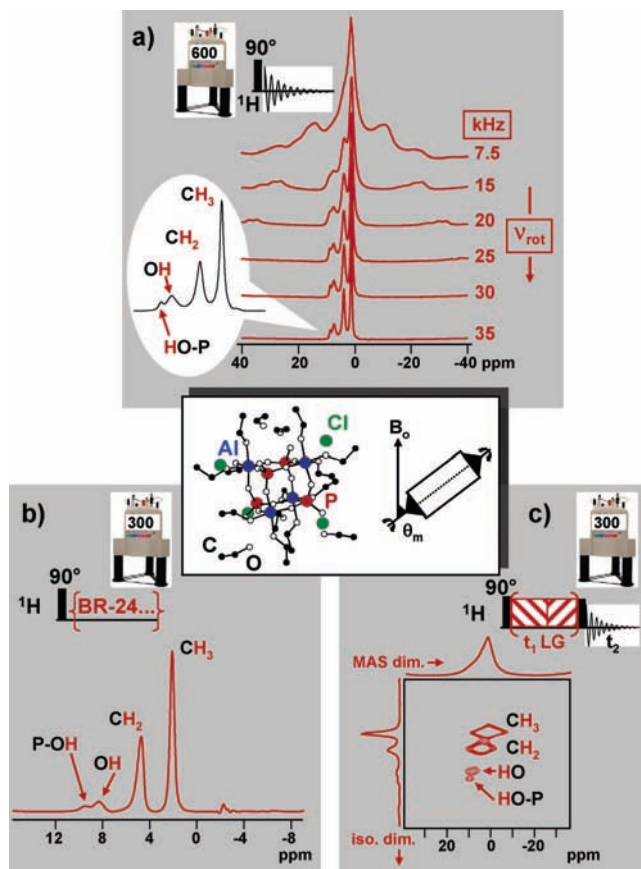
FIGURE 5. (a) ^{1}H MAS SPE for [Al$_4$(HPO$_4$)$_4$(C$_2$H$_5$OH)$_{12}$]Cl$_4$·4C$_2$H$_5$OH for variable ν_{rot} values. (b) CRAMPS-BR24 experiment. (c) ^{1}H–^{1}H correlation under LG irradiation.

When $\nu_{rot} = 35$ kHz, four isotropic resonances are observed corresponding to C$\underline{H}_3$C$\underline{H}_2$O$\underline{H}$ molecules and P–O$\underline{H}$ groups. The same resolution is obtained by using the CRAMPS-BR24 sequence[54] (Figure 5b), as well as in a 2D ^{1}H–^{1}H experiment under LG irradiation during t_1 (Figure 5c). Fast MAS at very high field is therefore an acceptable alternative for high-resolution ^{1}H NMR and has been widely used for the in-depth description of sol–gel materials and hybrid derivatives.[13–15,55]

Dipolar Interactions Assessed via CP, HETCOR, and BABA Experiments. The CP MAS experiment[8] increases the magnitude of the signal of the low-abundance nuclei (Y) from an abundant spin reservoir (X). It relies on the heteronuclear dipolar interaction, allowing therefore the measurement of distances between nuclei[56] and the study of local molecular motion. The basic CP MAS experiment is presented in Figure 6, involving three blocks. Block 1 corresponds to a t_1 evolution for X if 2D experiments are performed (HETCOR). Homonuclear decoupling between X nuclei can be applied. Block 2 corresponds to the CP transfer (during the contact time t_{CP}) under the Hartman–Hahn (H-H) condition.[57] Many improvements have been proposed for the efficient broadening of the H-H condition under very fast MAS.[58] LG irradiation of the X channel can be implemented as well. Block 3 corresponds to the acquisition of the Y signal under {X} decoupling. Spectacular improvements in terms of heteronuclear decoupling have recently been achieved.[59]
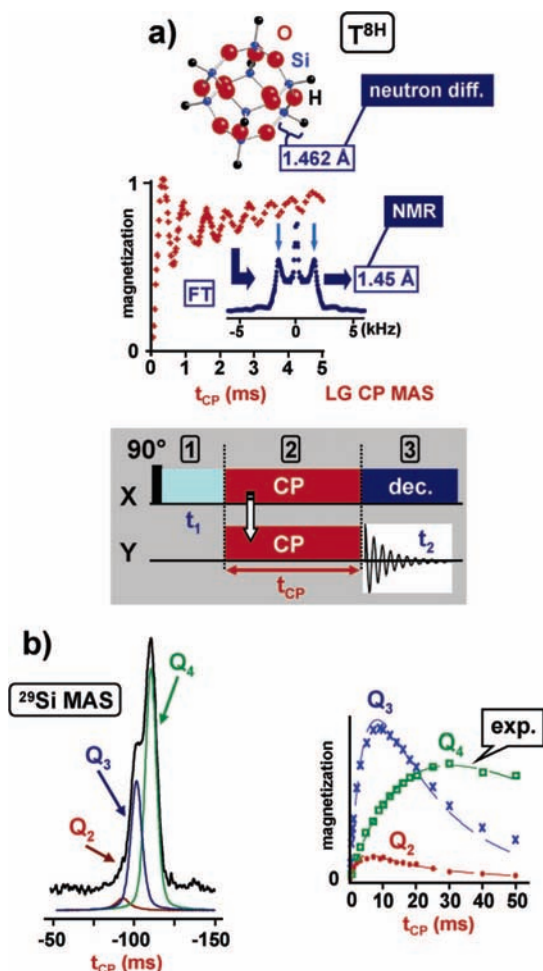
FIGURE 6. (a) ^{1}H–^{29}Si LGCP MAS experiment for T^{8H}. (b) ^{29}Si MAS spectrum of a silica-based xerogel. CP curves (vs t_{CP}) for the Q$_2$, Q$_3$, Q$_4$ units and the corresponding simulations at a fixed $T_{1\rho}{}^H$ of 20 ms.

Figure 6a shows the 1D ^{1}H–^{29}Si LGCP MAS magnetization versus t_{CP} for the {Si$_8$H$_8$O$_{12}$} T^{8H} silsesquioxane. Strong dipolar oscillations corresponding to the coherent transfer of magnetization are observed and subsequently Fourier-transformed. A pseudo-Pake doublet corresponding to a d_{Si-H} of 1.45 Å is obtained,[60] in very good agreement with neutron diffraction data.

The quantification of the CP experiment remains an open question: extreme care has to be taken when extracting quantitative data from CP curves (Figure 6b).[60,61] The fits of the CP dynamics curves for the Q$_i$ ($i = 2, 3$, or 4) sites present in silica and hybrid gels are generally based on the following equation:[8]

$$M_{^{29}Si}{}^{CP}(t_{CP}) = \gamma_{^1H}/|\gamma_{^{29}Si}| \; M_{^{29}Si} \; [1/(1-\lambda)] \; \times$$
$$[\exp(-t_{CP}/T_{1\rho}{}^H) - \exp(-t_{CP}/T_{HSi})] (1)$$

where $M_{^{29}Si}$ is the target and $\lambda = T_{HSi}/T_{1\rho}{}^H$ (T_{HSi}, cross-relaxation time constant; $T_{1\rho}{}^H$, ^{1}H relaxation time in the rotating frame). Usually, $\lambda \ll 1$ for Q$_2$ and Q$_3$ units in silica and hybrid gels. Quantitative data can then be extracted. For weakly coupled Q$_4$ sites, an independent measurement of $T_{1\rho}{}^H$ is necessary for the correct estimation of $M_{^{29}Si}$ by using eq 1 (Figure 6b). In the case of homogeneous TQ gels (involving both T and Q units), the direct

quantification of $M_{^{29}Si}$ for the Q$_4$ units is possible, as the protons of the T units efficiently cross polarize the Q$_4$ units.

A key NMR technique for investigating the organic–inorganic interfaces is the 2D ^{1}H–^{29}Si HETCOR sequence. Relevant examples can be found in the field of long-range ordered silica obtained through the self-assembly of a variety of amphiphilic templating agents with an inorganic phase generated through the sol–gel process. Chmelka et al. very nicely illustrated this by using ^{1}H–^{29}Si and ^{1}H–^{27}Al HETCOR experiments to investigate the distribution of PEO and PPO copolymer blocks within the silica matrix,[19] the aluminum incorporation in MCM-41 mesophases,[20] and the molecular proximities between the structure-directing surfactant molecules and the crystal-like silicate sheets in layered silicate surfactant mesophases.[21] The silica surfactant interactions in mesophases characterized by 2D hexagonal *p6m* symmetry and prepared with cetyltrimethylammonium bromide (CTAB) were investigated. The ^{1}H–^{29}Si HETCOR experiment recorded on the CTA$^+$–SiO$_2$ sample prepared under basic conditions (Figure 7a) shows clearly strong interactions between the positively charged polar head groups of the surfactant and the Si–O$^-$ surface sites (Q$_3$), as well as the fully condensed Q$_4$ sites. Correlations are even present between the protons of the surfactant chain and the Q$_3$ and Q$_4$ sites. From this analysis, a schematic model for the surfactant–silica interface can be proposed (Figure 7b).[62]

One can also use high-resolution ^{1}H MAS NMR to look for proximities between the Si surface sites and the template molecules. The most sensitive experiment for probing homonuclear dipolar couplings in solids is the DQ NMR experiment under fast MAS with recoupling schemes. The BABA sequence was used.[10,63] Templated silicas functionalized with vinyl groups have been studied in characterizing the location of the vinyl groups in the silica framework with respect to the polar head groups of the surfactant molecules (CTA$^+$). In the ^{1}H DQ experiment (Figure 8), coherences between the vinyl protons and the N(CH$_3$)$_3{}^+$ head group of CTA$^+$ molecules are observed, which clearly indicates that most of the vinyl groups are located at the surface. Interestingly, correlations are also observed between the vinyl protons and those of the alkyl chains. Reference 64 is an excellent review dealing with ^{1}H DQ spectroscopy in the context of macromolecular and supramolecular systems.

Finally, the CP process is strongly modulated by molecular motions and can become rather inefficient under some circumstances. Figure 9 presents the ^{13}C NMR study of entrapped ibuprofen molecules in MCM-41 materials[65] (host–guest system). Due to fast reorientation of the molecules, the ^{1}H–^{13}C CP efficiency is strongly reduced when compared to that in the ^{13}C MAS experiment. Therefore, HETCOR experiments cannot be performed in this particular case. At a low temperature (−50 °C), the rate of CP transfer obviously increases. A spectacular improvement in the signal-to-noise ratio is obtained by using the MAS-*J*-INEPT (insensitive nuclei enhanced by polarization transfer) sequence.[22] CP and
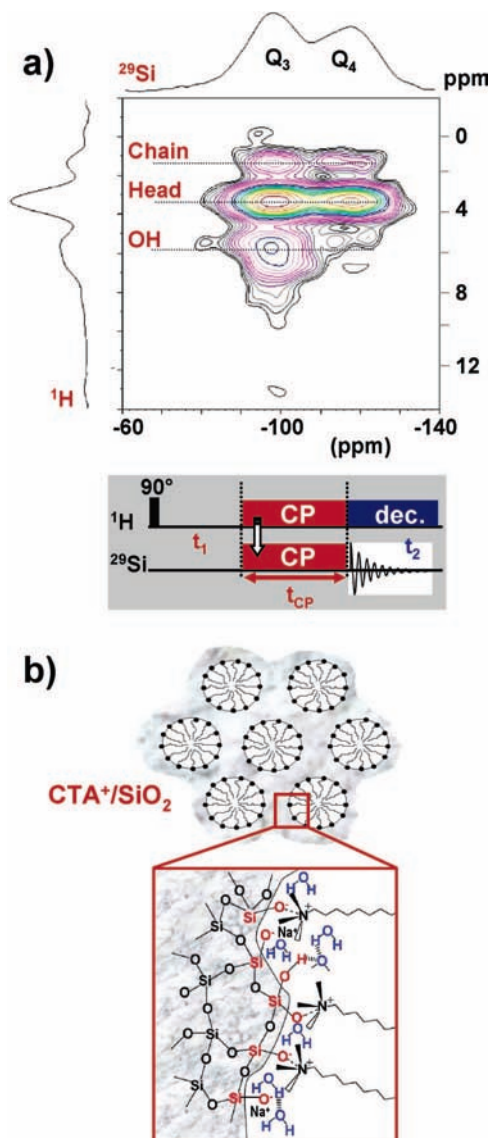
FIGURE 7. (a) ^1H–^{29}Si HETCOR experiment for a CTA^+–SiO_2 mesoporous derivative. (b) Schematic view of the interface interactions.[62]

J-derived techniques are complementary for the complete study of sol–gel-derived materials.

D-Mediated Experiments Involving Quadrupolar Nuclei. The setup of the CP MAS experiment involving ^1H and a quadrupolar nucleus (^{27}Al, ^{17}O, etc.)[66,67] must take into account the following points. (i) $T_{1\rho}^Q$ constants are usually small for quadrupolar nuclei, restricting t_{CP} to rather small values. Consequently, the signal-to-noise ratio can be very low. (ii) Low-power RF fields (down to a few kilohertz) are required on the quadrupolar channel for the manipulation of the central transition of the quadrupolar nucleus as a fictive $^1/_2$ spin.[68] Under such conditions, a pure quadrupolar line shape is obtained. Otherwise, deformed line shapes may be observed.

In Figure 10a, a pure second-order quadrupolar line shape is obtained via a 1D $^1H \rightarrow {}^{27}Al$ CP MAS experiment for the $[Al_4(HPO_4)_4(C_2H_5OH)_{12}]Cl_4 \cdot 4C_2H_5OH$ cluster (at $\nu_{^{27}Al} = 12.5$ kHz). The 2D LG HETCOR experiment with a small t_{CP} value (50 μs) shows a strong correlation signal
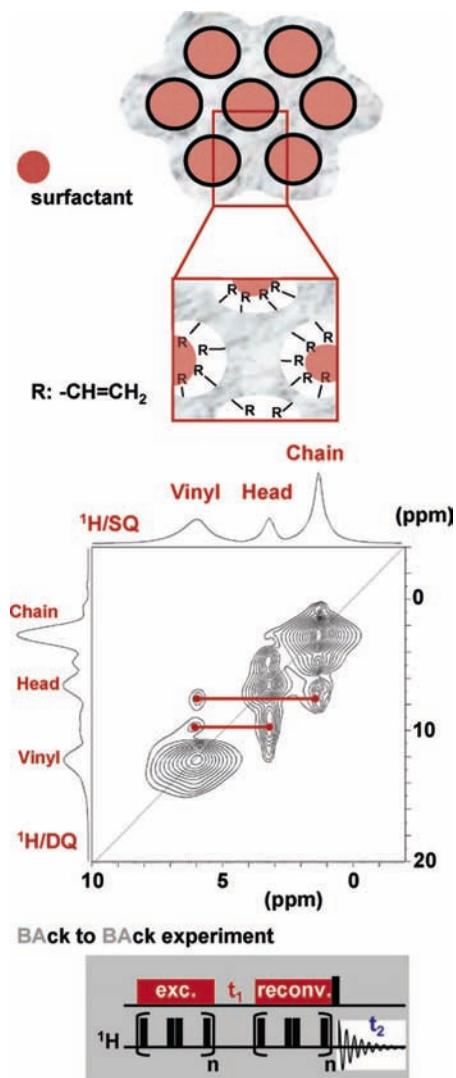

FIGURE 8. ^1H–^1H BABA sequence applied to vinyl-modified templated silica.

between aluminum and the proton signal at 8 ppm (OH groups of ethanol molecules). More dipolar connections are evidenced with larger t_{CP} values. These experiments show unambiguously that aluminum is coordinated to alcohol molecules and not to ethoxy groups.

In nonfavorable cases (very short $T_{1\rho}^Q$), the implementation of CP MAS experiments becomes almost impossible. The TRAPDOR experiment is a simple and robust alternative technique, which also relies on the heteronuclear dipolar interaction:[9,69] under MAS conditions, the dipolar interaction is reintroduced by applying a RF irradiation during the first τ period (where $\tau = k/\nu_{rot}$) of a spin echo experiment $90°-\tau-180°-\tau-$acq (Figure 10b). Consequently, the magnitude of the signal of the observed nucleus decreases when compared to that in the same experience without irradiation, as soon as the detected and irradiated nuclei are close in space. Usually, the analysis is done by plotting $(I_0 - I)/I_0$ (where I and I_0 are the signal intensities with and without irradiation, respectively) versus τ. An example of phase identification through the TRAPDOR approach is shown in Figure 10b. The minor peak in the ^{31}P MAS spectrum of a silica–hydroxyapatite composite
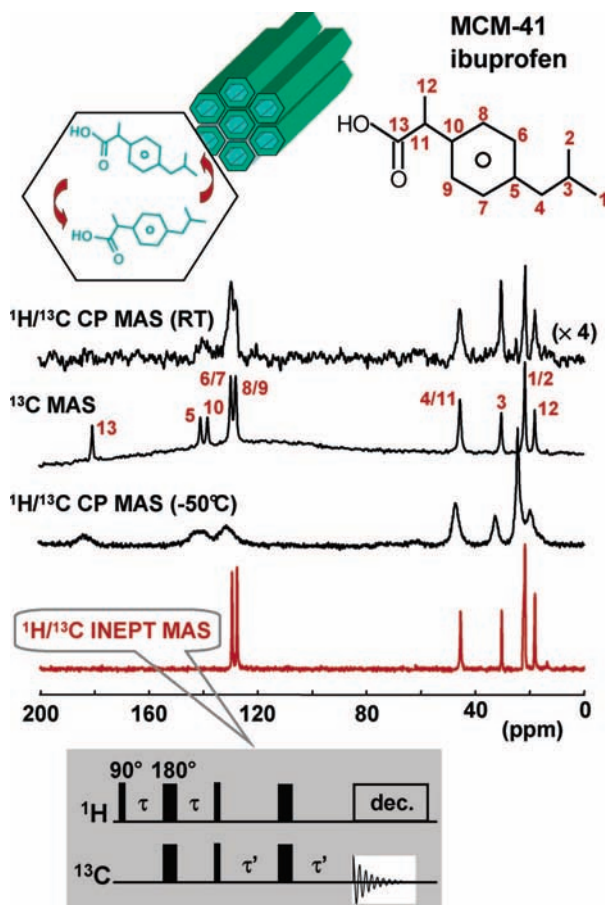
FIGURE 9. ^{13}C NMR study of ibuprofen molecules entrapped in MCM-41 silica: MAS, [1]H–[13]C CP MAS (at room temperature and −50 °C), and [1]H–[13]C MAS-*J*-INEPT.

is assigned to $NaCaPO_4$ which is submitted to a strong $\{^{23}Na\}$–[31]P TRAPDOR effect.[70] This is not the case for the ^{31}P sites of the silica–HAP composite.

First-Principles Calculations of NMR Parameters

Interpretation of high-resolution spectra can be a difficult task, and in this context, first-principles calculations can be extremely useful in providing accurate calculation of the NMR parameters.

The quantum mechanical calculation of NMR parameters involving a detailed description of the electrons and nuclei in the presence of B_0 is a complex many-body problem needing approximations.[11] Density functional theory (DFT) can be employed where the energy is considered as a functional of the total charge density. A possibility for describing infinite solids implies their approximation by clusters which are terminated with nuclei such as [1]H. Alternative approaches involve the use of periodic boundary conditions. Pickard and Mauri[11] introduced a plane wave pseudopotential method for calculating NMR parameters, and the calculated parameters for a variety of silica polymorphs were shown to be in excellent agreement with experimental data.[71]

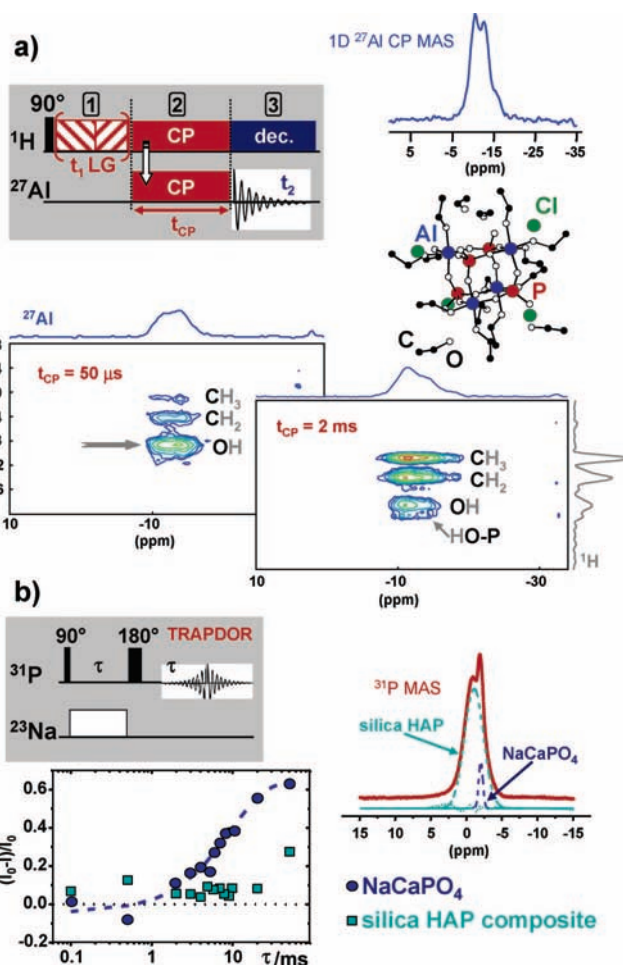First-principles computations require a precise structure to be calculated, but sol–gel-derived oxide networks

FIGURE 10. (a) [1]H–[27]Al LGCP MAS experiment for $[Al_4(HPO_4)_4$-$(C_2H_5OH)_{12}]Cl_4 \cdot 4C_2H_5OH$ for variable t_{CP} values. (b) [31]P–[23]Na TRAPDOR experiment for a silica HAP composite.

are not usually well ordered. Nevertheless, the structure of a surfactant-templated silicate framework without 3D crystallinity could be established by using a combination of solid state NMR spectroscopy, XRD, first-principles calculations, and extensive modeling.[12] Comparison between experimental and calculated ^{29}Si NMR parameters allowed confirmation of the proposed structure.

Conclusions

Solid state NMR offers a unique array of techniques allowing the precise characterization of interfaces in sol–gel-derived materials. All NMR interactions, ranging from the isotropic chemical shift to the quadrupolar interaction, can be used as spectroscopic spies. The key experiments correspond to high-resolution techniques, such as MAS and MQ MAS. Under fast reorientation of the samples, a resolved dimension is usually obtained, in connection with other spectral dimensions related to the anisotropy of the interactions. We have shown that δ and *J* parameters are able to establish chemical connectivities between the nuclei, leading to the notion of chemical homogeneity at a molecular level. Dipolar interactions can establish spatial connectivities which are of prime importance for the description of hybrid interfaces.

We believe that in the near future, spectacular improvements in solid state NMR concepts and experiments will emerge, leading to an even higher-performance approach for investigation. The first-principles calculation of NMR parameters for amorphous interfaces remains an exciting challenge.

References

(1) Sanchez, C.; Soller-Illia, G. J. A. A.; Ribot, F.; Lalot, T.; Mayer, C. R.; Cabuil, V. Designed hybrid organic-inorganic nanocomposites from functional nanobuilding blocks. *Chem. Mater.* **2001**, *13*, 3061–3083.

(2) Massiot, D. High resolution solid state NMR. In *High Magnetic Fields Applied in Condensed Matter, Physics and Spectroscopy*; Berthier, C., et al., Eds.; Springer-Verlag: Heidelberg, Germany, 2002; CNP Vol. *595*.

(3) Epping, J. D.; Chmelka, B. F. Nucleation and growth of zeolites and inorganic mesoporous solids: Molecular insights from magnetic resonance spectroscopy. *Curr. Opin. Colloid Interface Sci.* **2006**, *11*, 81–117.

(4) Frydman, L.; Harwood, J. S. Isotropic spectra of half-integer quadrupolar spins from bidimensional Magic Angle Spinning NMR. *J. Am. Chem. Soc.* **1995**, *117*, 5367–5368.

(5) Samoson, A.; Tuherm, T.; Gan, Z. High field high speed MAS resolution enhancement in ^{1}H NMR spectroscopy of solids. *Solid State NMR* **2001**, *20*, 130–136.

(6) Fyfe, C. A.; Feng, Y.; Gies, H.; Grondey, H.; Kokotailo, G. T. Natural-abundance two-dimensional solid-state silicon-29 NMR investigations of three-dimensional lattice connectivities in zeolite structures. *J. Am. Chem. Soc.* **1990**, *112*, 3264–3270.

(7) Massiot, D.; Fayon, F.; Alonso, B.; Trebosc, J.; Amoureux, J. P. Chemical bonding differences evidenced from J-coupling in solid state NMR experiments involving quadrupolar nuclei. *J. Magn. Reson.* **2003**, *164*, 160–164.

(8) Pines, A.; Gibby, M. G.; Waugh, J. S. Proton-enhanced NMR of dilute spins in solids. *J. Chem. Phys.* **1973**, *59*, 569–590.

(9) Grey, C. P.; Vega, A. J. Determination of the quadrupole coupling constant of the invisible aluminum spins in zeolite HY with ^{1}H/^{27}Al TRAPDOR NMR. *J. Am. Chem. Soc.* **1995**, *117*, 8232–8242.

(10) Feike, M.; Demco, D. E.; Graf, R.; Gottwald, J.; Hafner, S.; Spiess, H. W. Broadband multiple-quantum NMR spectroscopy. *J. Magn. Reson., Ser. A* **1996**, *122*, 214–221.

(11) Pickard, C. J.; Mauri, F. In *Calculation of NMR and EPR Parameters: Theory and Applications*; Knaupp, M., Ed.; Wiley-VCH: Weinheim, Germany, 2004; see also references therein.

(12) Hedin, N.; Graf, R.; Christiansen, S. C.; Gervais, C.; Hayward, R. C.; Eckert, J.; Chmelka, B. F. Structure of a surfactant-templated silicate framework in the absence of 3D crystallinity. *J. Am. Chem. Soc.* **2004**, *126*, 9425–9432.

(13) Alonso, B.; Massiot, D.; Babonneau, F.; Brusatin, G.; Della Giustina, G.; Kidchob, T.; Innocenzi, P. Structural control in germania hybrid organic-inorganic materials. *Chem. Mater.* **2005**, *17*, 3172–3180.

(14) Brus, J.; Dybal, J. Hydrogen-bond interactions in organically-modified polysiloxane networks studied by 1D and 2D CRAMPS and double-quantum ^{1}H MAS NMR. *Macromolecules* **2002**, *35*, 10038–10047.

(15) Camus, L.; Goletto, V.; Maquet, J.; Gervais, C.; Bonhomme, C.; Babonneau, F. ^{1}H MAS-NMR at high spinning rate: An interesting characterization tool for hybrid materials. *J. Sol-Gel Sci. Technol.* **2003**, *26*, 311–314.

(16) Babonneau, F.; Bonhomme, C.; Gervais, C.; Maquet, J. Advances in characterization methods for sol-gel derived materials: High resolution solid state nuclear magnetic resonance. *J. Sol-Gel Sci. Technol.* **2004**, *31*, 9–17.

(17) Brus, J.; Spirkova, M.; Hlavata, D.; Strachota, A. Self-organization, structure, dynamic properties, and surface morphology of silica/epoxy films as seen by solid state NMR, SAXS, and AFM. *Macromolecules* **2004**, *37*, 1346–1357.

(18) Saalwächter, K.; Krause, M.; Gronski, W. Study of molecular interactions and dynamics in thin silica surface layers by proton solid state NMR spectroscopy. *Chem. Mater.* **2004**, *16*, 4071–4079.

(19) Janicke, M. T.; Landry, C. C.; Christiansen, S. C.; Kumar, D.; Stucky, G. D.; Chmelka, B. F. Aluminum incorporation and interfacial structures in MCM-41 mesoporous molecular sieves. *J. Am. Chem. Soc.* **1998**, *120*, 6940–6951.

(20) Janicke, M. T.; Landry, C. C.; Christiansen, S. C.; Birtalan, S.; Stucky, G. D.; Chmelka, B. F. Low silica MCM-41 composites and mesoporous solids. *Chem. Mater.* **1999**, *11*, 1342–1351.

(21) Christiansen, S. C.; Zhao, D.; Janicke, M. T.; Landry, C. C.; Stucky, G. D.; Chmelka, B. F. Molecularly ordered inorganic frameworks in layered silicate surfactant mesophases. *J. Am. Chem. Soc.* **2001**, *123*, 4519–4529.

(22) Alonso, B.; Massiot, D. Multi-scale NMR characterisation of meso-structured materials using ^{1}H $\rightarrow$ ^{13}C through-bond polarisation transfer, fast MAS, and ^{1}H spin diffusion. *J. Magn. Reson.* **2003**, *163*, 347–352.

(23) Trebosc, J.; Wiench, J. W.; Huh, S.; Lin, V. S. Y.; Pruski, M. Studies of organically functionalized mesoporous silicas using hetero-nuclear solid state correlation NMR spectroscopy under fast magic angle spinning. *J. Am. Chem. Soc.* **2005**, *127*, 7587–7593.

(24) De Paul, S. M.; Zwanziger, J. W.; Ulrich, R.; Wiesner, U.; Spiess, H. W. Structure, mobility, and interface characterization of self-organized organic-inorganic hybrid materials by solid-state NMR. *J. Am. Chem. Soc.* **1999**, *121*, 5727–5736.

(25) Alam, T. M.; Fan, H. Investigation of templated mesoporous silicate thin films using high speed, solid-state ^{1}H MAS and double quantum NMR spectroscopy. *Macromol. Chem. Phys.* **2003**, *204*, 2023–2030.

(26) Sizun, C.; Raya, J.; Intasiri, A.; Boos, A.; Elbayed, K. Investigation of the surfactants in CTAB-templated mesoporous silica by ^{1}H HRMAS NMR. *Microporous Mesoporous Mater.* **2003**, *66*, 27–36.

(27) Tiemann, M.; Fröba, M. Mesoporous aluminophosphates from a single source precursor. *Chem. Commun.* **2002**, 406–407.

(28) Zhang, C.; Babonneau, F.; Bonhomme, C.; Laine, R. M.; Soles, C. L.; Hristov, H. A.; Yee, A. F. Highly porous polyhedral silsesquioxane polymers. Synthesis and characterization. *J. Am. Chem. Soc.* **1998**, *120*, 8380–8391.

(29) Laine, R. M. Nanobuilding blocks based on the $[OSiO_{1.5}]_x$ (x = 6, 8, 10) octasilsesquioxanes. *J. Mater. Chem.* **2005**, *15*, 3725–3744.

(30) Ashbrook, S. E.; Smith, M. E. Solid state ^{17}O NMR: An introduction to the background principles and applications to inorganic materials. *Chem. Soc. Rev.* **2006**, *35*, 718–735.

(31) Walter, T. M.; Turner, G. L.; Oldfield, E. Oxygen-17 cross-polarization NMR spectroscopy of inorganic solids. *J. Magn. Reson.* **1988**, *76*, 106–120.

(32) Bastow, T. J.; Moodie, A. F.; Smith, M. E.; Whitfield, H. J. Characterisation of titania gels by ^{17}O nuclear magnetic resonance and electron diffraction. *J. Mater. Chem.* **1993**, *3*, 697–702.

(33) Guermeur, C.; Lambard, J.; Gerard, J.-F.; Sanchez, C. Hybrid polydimethylsiloxane zirconium oxo nanocomposites. Characterization of the matrix and the siloxane-zirconium oxo interface. *J. Mater. Chem.* **1999**, *9*, 769–778.

(34) Pickup, D. M.; Mountjoy, G.; Holland, M. A.; Wallidge, G. W.; Newport, R. J.; Smith, M. E. Structure of $(Ta_2O_5)_x(SiO_2)_{1-x}$ xerogels (x = 0.05, 0.11, 0.18, 0.25 and 1.0) from FTIR, ^{29}Si and ^{17}O MAS NMR and EXAFS. *J. Mater. Chem.* **2000**, *10*, 1887–1894.

(35) Filowitz, M.; Ho, R. K. C.; Klemperer, W. G.; Shum, W. Oxygen-17 nuclear magnetic resonance spectroscopy of polyoxometalates. 1. Sensitivity and resolution. *Inorg. Chem.* **1979**, *18*, 93–103.

(36) Hussin, R.; Dupree, R.; Holland, D. The Ge-O-Ge bond angle distribution in GeO_2 glass: A NMR determination. *J. Non-Cryst. Solids* **1999**, *246*, 159–168.

(37) Pozarnsky, G. A.; McCormick, A. V. ^{17}O nuclear magnetic resonance spectroscopy of the structural evolution of vanadium pentaoxide gels. *J. Mater. Chem.* **1994**, *4*, 1749–1753.

(38) Dirken, P. J.; Kohn, S. C.; Smith, M. E.; van Eck, E. R. H. Complete resolution of Si-O-Si and Si-O-Al fragments in an aluminosilicate glass by ^{17}O multiple quantum magic angle spinning NMR spectroscopy. *Chem. Phys. Lett.* **1997**, *266*, 568–574.

(39) Wang, S.; Stebbins, J. F. Multiple-quantum magic-angle spinning ^{17}O NMR studies of borate, borosilicate, and boroaluminate glasses. *J. Am. Ceram. Soc.* **1999**, *82*, 1519–1528.

(40) Dirken, P. J.; Smith, M. E.; Whitfield, H. J. ^{17}O and ^{29}Si solid state NMR study of atomic scale structure in sol-gel-prepared TiO_2-SiO_2 materials. *J. Phys. Chem.* **1995**, *99*, 395–401.

(41) Gervais, C.; Babonneau, F.; Smith, M. E. Detection, quantification, and magnetic field dependence of solid-state ^{17}O NMR of X-O-Y (X,Y = Si,Ti) linkages: Implications for characterizing amorphous titania-silica-based materials. *J. Phys. Chem. B* **2001**, *105*, 1971–1977.

(42) Alonso, B.; Sanchez, C. Structural investigation of polydimethyl-siloxane-vanadate hybrid materials. *J. Mater. Chem.* **2000**, *10*, 377–386.

(43) Babonneau, F.; Maquet, J. Nuclear magnetic resonance techniques for the structural characterization of siloxane-oxide hybrid materials. *Polyhedron* **2000**, *19*, 315–322.

(44) Julian, B.; Gervais, C.; Rager, M.-N.; Maquet, J.; Cordoncillo, E.; Escribano, P.; Babonneau, F.; Sanchez, C. Solid-state ^{17}O NMR characterization of PDMS-MxOy (M = Ge(IV), Ti(IV), Zr(IV), Nb(V), and Ta(V)) organic-inorganic nanocomposites. *Chem. Mater.* **2004**, *16*, 521–529.

(45) Lafond, V.; Gervais, C.; Maquet, J.; Prochnow, D.; Babonneau, F.; Mutin, P. H. ^{17}O MAS NMR study of the bonding mode of phosphonate coupling molecules in a titanium oxo-alkoxo-phosphonate and in titania-based hybrid materials. *Chem. Mater.* **2003**, *15*, 4098–4103.

(46) Cadars, S.; Lesage, A.; Emsley, L. Chemical shift correlations in disordered solids. *J. Am. Chem. Soc.* **2005**, *127*, 4466–4476.

(47) (a) Fayon, F.; Roiland, C.; Emsley, L.; Massiot, D. Triple-quantum correlation NMR experiments in solids using *J*-couplings. *J. Magn. Reson.* **2006**, *179*, 49–57. (b) Fayon, F.; Massiot, D.; Levitt, M. H.; Titman, J. J.; Gregory, D. H.; Duma, L.; Emsley, L.; Brown, S. P. Through-space contributions to two-dimensional double-quantum J correlation NMR spectra of Magic-Angle-Spinning solids. *J. Chem. Phys.* **2005**, *122*, 194313-1–14.

(48) Coelho, C.; Babonneau, F.; Azaïs, T.; Bonhomme-Coury, L.; Maquet, J.; Laurent, G.; Bonhomme, C. Chemical bonding in silicophosphate gels: Contribution of dipolar and J-derived solid state NMR techniques. *J. Sol-Gel Sci. Technol.* **2006**, *40*, 181–189.

(49) Coelho, C.; Azaïs, T.; Bonhomme-Coury, L.; Maquet, J.; Massiot, D.; Bonhomme, C. Application of the MAS-J-HMQC experiment to a new pair of nuclei {^{29}Si,^{31}P}: Si$_5$O(PO$_4$)$_6$ and SiP$_2$O$_7$ polymorphs. *J. Magn. Reson.* **2006**, *179*, 114–119.

(50) Azaïs, T.; Bonhomme, C.; Bonhomme-Coury, L.; Vaissermann, J.; Millot, Y.; Man, P. P.; Bertani, P.; Hirschinger, J.; Livage, J. Cubane shaped clusters, precursors for aluminophosphate frameworks: A solid state multinuclear NMR study, in time and frequency domains. *J. Chem. Soc., Dalton Trans.* **2002**, 609–618.

(51) Van Rossum, B. J.; De Groot, C. P.; Ladizhansky, V.; Vega, S.; De Groot, H. J. M. A method for measuring heteronuclear (^{1}H-^{13}C) distances in high speed MAS NMR. *J. Am. Chem. Soc.* **2000**, *122*, 3465–3472.

(52) Gerstein, B. C.; Pembleton, R. G.; Wilson, R. C. High resolution NMR in randomly oriented solids with homonuclear dipolar broadening: Combined multiple pulse NMR and Magic Angle Spinning. *J. Chem. Phys.* **1977**, *66*, 361–362.

(53) Elena, B.; De Paëpe, G.; Emsley, L. Direct spectral optimisation of proton-proton homonuclear dipolar decoupling in solid-state NMR. *Chem. Phys. Lett.* **2004**, *398*, 532–538.

(54) Burum, D. P.; Rhim, W. K. Analysis of multiple pulse NMR in solids. III. *J. Chem. Phys.* **1979**, *71*, 944–956.

(55) Massiot, D.; Alonso, B.; Fayon, F.; Fredoueil, F.; Bujoli, B. New NMR developments for structural investigation of proton-bearing materials at different length scales. *Solid State Sci.* **2001**, *3*, 11–16.

(56) Azaïs, T.; Bonhomme-Coury, L.; Vaissermann, J.; Bertani, P.; Hirschinger, J.; Maquet, J.; Bonhomme, C. Synthesis and characterization of a novel cyclic aluminophosphinate: Structure and solid-state NMR study. *Inorg. Chem.* **2002**, *41*, 981–988.

(57) Hartmann, S. R.; Hahn, E. L. Nuclear double resonance in the rotating frame. *Phys. Rev.* **1962**, *128*, 2042–2053.

(58) Christiansen, S. C.; Hedin, N.; Epping, J. D.; Janicke, M. T.; del Amo, Y.; Demarest, M.; Brzezinski, M.; Chmelka, B. F. Sensitivity considerations in polarization transfer and filtering using dipole-dipole couplings: Implications for biomineral systems. *Solid State NMR* **2006**, *29*, 170–182.

(59) Ernst, M. Heteronuclear spin decoupling in solid-state NMR under Magic-Angle Sample spinning. *J. Magn. Reson.* **2003**, *162*, 1–34.

(60) Bonhomme, C.; Camus, L.; Babonneau, F. Silica and hybrid silica gels revisited: New insight by solid state nuclear magnetic resonance. *Mater. Res. Symp. Proc.* **2005**, *847*, EE4.6.1–11.

(61) Klur, I.; Jacquinot, J. F.; Brunet, F.; Charpentier, T.; Virlet, J.; Schneider, C.; Tekely, P. NMR cross-polarization when $T_{IS} > T_{1r}$: Examples from silica gel and calcium silicate hydrates. *J. Phys. Chem. B* **2000**, *104*, 10162–10167.

(62) Baccile, N.; Maquet, J.; Babonneau, F. Investigation by ^{1}H–^{29}Si HETCOR NMR experiments of surfactant/silica interfaces in mesostructured materials with ordered porosity. *C. R. Chim.* **2006**, *9*, 478–484.

(63) Schnell, I.; Spiess, H. W. High-resolution ^{1}H NMR spectroscopy in the solid state: Very fast sample rotation and multiple-quantum coherences. *J. Magn. Reson.* **2001**, *151*, 153–227.

(64) Brown, S. P.; Spiess, H. W. Advanced solid-state NMR methods for the elucidation of structure and dynamics of molecular, macromolecular, and supramolecular systems. *Chem. Rev.* **2001**, *101*, 4125–4157.

(65) Azaïs, T.; Tourné-Péteilh, C.; Aussenac, F.; Baccile, N.; Coelho, C.; Devoisselle, J. M.; Babonneau, F. Solid state NMR study of ibuprofen confined in MCM-41 material. *Chem. Mater.* **2006**, *18*, 6382–6390.

(66) Woessner, D. E. Observation of effects of hydration on CP/MAS NMR measurements on quadrupolar nuclei. *Z. Phys. Chem.* **1987**, *152*, 51–58.

(67) Morris, H. D.; Ellis, P. D. ^{27}Al cross polarization of aluminas. The NMR spectroscopy of surface aluminum atoms. *J. Am. Chem. Soc.* **1989**, *111*, 6045–6049.

(68) Barrie, P. J. Distorted powder lineshapes in ^{27}Al CP/MAS NMR spectroscopy of solids. *Chem. Phys. Lett.* **1993**, *208*, 486–490.

(69) van Eck, E. R. H.; Janssen, R.; Maas, W. E. J. R.; Veeman, W. S. A novel application of nuclear spin-echo double-resonance to aluminophosphates and aluminosilicates. *Chem. Phys. Lett.* **1990**, *174*, 428–432.

(70) Andersson, J.; Johannessen, E.; Areva, S.; Baccile, N.; Azaïs, T.; Lindén, M. Physical properties and *in vitro* bioactivity of hierarchical porous silica/HAP composites. *J. Mater. Chem.* **2007**, *17*, 463–468.

(71) Profeta, M.; Mauri, F.; Pickard, C. J. Accurate first principles prediction of ^{17}O NMR parameters in SiO$_2$: Assignment of the zeolite ferrierite spectrum. *J. Am. Chem. Soc.* **2003**, *125*, 541–548.

AR600030J